NEW DEVELOPMENT ON SHAPE MEMORY ALLOYS ACTUATORS

Roberto Romano
Instituto de Pesquisas Tecnológicas do Estado de São Paulo and Telecommunications and Control Department
Escola Politécnica da Universidade de São Paulo, São Paulo, Brazil

Eduardo Aoun Tannuri
Instituto de Pesquisas Tecnológicas do Estado de São Paulo and Mechatronics Engineering Department
Escola Politécnica da Universidade de São Paulo, São Paulo, Brazil

Keywords: Modeling, shape memory alloy, actuator, robotics, sliding mode control.

Abstract: The present paper presents the development of a mechanical actuator using a shape memory alloy with a novel cooling system based on the thermo-electric effect (Seebeck-Peltier effect). Such a method has the advantage of reduced weight and requires a simpler control strategy as compared to other forced cooling systems. A complete mathematical model of the actuator was derived, and an experimental prototype was implemented. Several experiments are used to validate the model and to identify all parameters. A robust and nonlinear controller, based on sliding-mode theory, was derived and implemented. Experiments were used to evaluate the actuator closed-loop performance, stability, and robustness properties. The results showed that the proposed cooling system is able to improve the dynamic response of the actuator.

1 INTRODUCTION

Shape Memory Alloys (SMAs) consist of a group of metallic materials that demonstrate the ability to return to some previously defined shape or size when subjected to the appropriate thermal procedure. The shape memory effect occurs due to a temperature and stress dependent shift in the materials crystalline structure between two different phases called Martensite and Austenite. Martensite, the low temperature phase, is relatively soft whereas Austenite, the high temperature phase, is relatively hard. The change that occurs within SMAs crystalline structure is not a thermodynamically reversible process and results in temperature hysteresis. SMAs have been used in a variety of actuation applications. The key feature of this material is its ability to undergo large seemingly strains and subsequently recover these strains when a load is removed or the material is heated. SMA actuators have several advantages such as excellent power to mass ratio, maintainability, reliability, and clean and silent actuation. The disadvantages are low energy efficiency due to conversion of heat to mechanical energy, inaccurate motion control due to hysteresis, nonlinearities, parameter uncertainties, difficulty in measuring variables such as temperature and the slow response due to the thermal process evolved in the working principle.

To operate quickly, the SMA must be cooled rapidly. Some researchers have proposed static methods, in which the SMA wires are continually cooled by means of an air stream (Tanaka and Yamada, 1991). In a similar way, Furuya and Shimada (1990) used a cooling system based on water immersion. In such case, cooling time was reduced in 10 times compared to a non-cooled wire. However, the power consumption of such actuator has increased by a factor of 20, since in the heating phase it is necessary much more power to compensate the heat that is lost by the cooling system. Golbert and Russel (1995) used a mobile metallic heat sink and a complex mechanism guaranteed that the sink was only in contact to the wire being cooled, which minimizes the power consumption of the actuator and increases its dynamic behavior. Asada and Mascaro (2002) developed an actuator with a cooling system based on flowing water around the wire. A complex

Romano R. and Aoun Tannuri E. (2008).
NEW DEVELOPMENT ON SHAPE MEMORY ALLOYS ACTUATORS.
In *Proceedings of the First International Conference on Biomedical Electronics and Devices*, pages 55-61
DOI: 10.5220/0001047800550061

system guarantees that water flows only when wire must be cooled. The dynamic response of the actuator is expressively better, and the power consumption is also acceptable.In order to increase the dynamic characteristics of SMA actuators, keeping a simple mechanical and electrical design, the present work proposes a novel cooling system based on thermoelectric effect (Seebeck-Peltier effect). A complete mathematical model of the actuator is derived and an experimental prototype is used to validate the model and identify all parameters. A sliding-mode control is also derived and some preliminarily results of its application in the experimental system are obtained and discussed.

2 EXPERIMENTAL SET-UP

An experimental prototype of the SMA actuator, cooled by a thermoelectric element, was built. It was used to validate the mathematical model and to evaluate the control algorithm. Figure 1 shows a simple scheme of the actuator. The thermoelectric tablet is assembled in a heat sink and a small blower is also used to dissipate the heat. The SMA wire is attached to the structure, by means of an electric connector C1. The other end of the wire is attached to the intern pulley (radius r1=0.45cm). A 40g load is supported by a wire connected to the external pulley (r2=4.5cm). The length of the SMA wire is 15cm, and its typical 4.0% deformation is amplified by a factor 10. So, it is expected a 6cm elevation of the load, which is equivalent to a 76^0 pulley rotation. Such rotation is measured by a potentiometer directly attached to the pulley axis.

Figure 2 shows a picture of the actuator. The signal conditioning module is composed by a constant current amplifier that supplies up to 1A the electric current to heat the SMA wire and by a voltage amplifier/filter connected to the potentiometer.

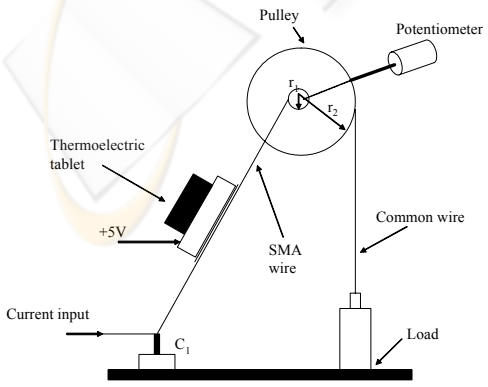

Figure 1: Diagram of the SMA actuator.

The module is connected to a computer (Pentium 100MHz) by mean of a 10bits AD/DA board. The thermoelectric tablet is constantly powered by a 5V tension.

A Matlab/Simulink software was used to acquire and process the data from the potentiometer, and to send the command to the current that must be imposed to the SMA wire. Such software is flexible, and several control algorithms can be easily implemented. Furthermore, all graphical and mathematical tools provided by Matlab/Simulink can be used. The interface with AD/DA board was developed by means of a low-level code included in the software.

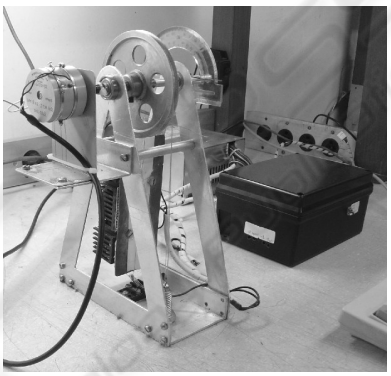

Figure 2: Picture of the actuator.

3 MATHEMATICAL MODEL

The model developed in the present work is based on the formulations proposed by Ikuta, Tsukamoto and Hirose (1991); Grant, Hayward and Lu (1997); Ashrafiuon and Elahinia (2002), Hoder, Vasina and Solc (2003) and Dutta and Ghorbel (2005). It is composed by a thermal model, a phase transformation model and a description of the mechanical properties and dynamics of the system (Figure 3).

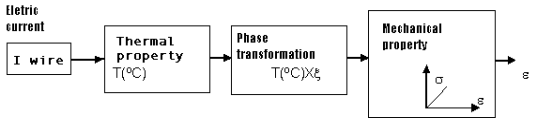

Figure 3: SMA actuator model.

The main variables used in the model are:

i – electric current in the SMA wire (A)
T – SMA wire temperature (ºC)
ξ - martensite fraction (0 a 100%)
σ - mechanical stress in the SMA wire (N/m^2)
ε - deformation (strain) of the SMA wire ($\Delta L/L$)

3.1 Thermal Model

Thermal model was base on the system shown in Figure 4 in which the SMA wire touches the thermoelectric element. The temperature of the element is considered to be constant, equal to 15 ^{0}C.

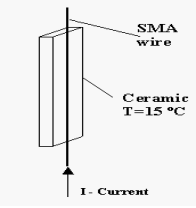

Figure 4: SMA wire and cooling element.

Considering several simplification hypothesis (Grand, Hayward and Lu, 1997), the thermal model can be written as (thermomechanical coupling is also not included since the deformation rate of the SMA wire is small, and such effect becomes important for fast or highly oscillatory deformations):

$$m.c_p.\frac{dT}{dt} = i^2.R - h.A.(T - T_{amb}.) - C.(T - T_p) \qquad (1)$$

In the previous equation, T_p is the temperature on the surface of the cooling element (15^{o}C), T_{amb} is the ambient temperature (considered to be 20^{o}C), h is the natural convection coefficient per unity length of SMA wire (in W/m^2 ºC/m) and C is the conduction coefficient per unity length (in W/ ºC/m). Furthermore, technical specifications of the SMA wire Flexinol FLX 00870, 0.008'', 70ºC) are given by (Dynalloy, 2005):

m - mass per unity length (2.10^{-4} Kg/m)
c_p - specific heat (837 J/Kg.K)
R - electrical resistance per unity length (32Ω/m)
A - external area per unity length (6.28.10^{-4} m^2/m)
d -diameter (2.10^{-4}m)

The parameters h and C are very difficult to estimate, since they depend on several variables. A rough estimation of such parameters, based on the theory exposed in Incropera and Witt (1998), are C = 0.4 W/ºC/m and h=6.55 W/m^{2}ºC/m. In the sequel, an identification procedure will be used to obtain values closer to the real ones.

3.2 Phase Transformation

During heating, occurs the transformation between Martensite (M) to Austenite (A), and during the cooling phase, the opposite transformation occurs. Basic equations that model such transformations, as a function of temperature, are given below (Ikuta, Tsukamoto and Hirose, 1991):

$$\xi = \frac{\xi_m}{1 + \exp\left[\frac{6.2}{Af - As}\left(T - \frac{As + Af}{2}\right)\right]} \quad \text{(heating)}$$

$$\xi = \frac{1 - \xi_A}{1 + \exp\left[\frac{6.2}{Mf - Ms}\left(T - \frac{Ms + Mf}{2}\right)\right]} + \xi_A \quad \text{(cooling)} \qquad (2)$$

where As and Af are the initial and final temperature of austenite transformation respectively; Ms and Mf are the initial and final temperature of martensite transformation respectively, ξ_m is the highest martensite fraction during cooling and ξ_A is the initial value of martensite fraction during cooling. Typical values are As=68ºC, Af= 78ºC, Ms=52ºC and Mf= 42ºC (Dynalloy, 2005). However, such values may present variations up to ±15^{o}C, and an identification procedure will be applied to evaluate the correct values for the wire used in the experimental actuator. Phase transformation is shown in Figure 5, and the hysteresis gets evident (Holder; Solc and Vasina, 2003).

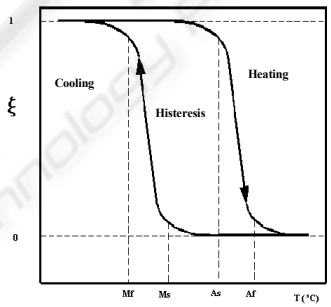

Figure 5: Phase transformation plot.

3.3 Mechanical Properties and Dynamics

Mechanical properties of shape memory alloys are obtained by means of a multiple layer model. The austenite phase is characterized by an elastic behavior. The martensite phase presents a behavior that seems to be plastic, deformed by a small stress (Ikuta, Tsukamoto and Hirose, 1991). So, for ξ= 0 (full austenite), the stress-strain relation is given by:

$$\sigma_A = E_A.\varepsilon \qquad (3)$$

where σ_A is the mechanical stress in the austenite portion of the alloy and E_A is the austenite Young's Modulus. In the other way, when ξ = 1 (full martensite), the stress-stain relation is given by:

$$\begin{aligned} \sigma_m &= E_m.\varepsilon \quad \text{if} \quad |\varepsilon| \le |\varepsilon_{my}| \\ \sigma_m &= E_m.\varepsilon_{my} \quad \text{if} \quad |\varepsilon| > |\varepsilon_{my}| \end{aligned} \qquad (4)$$

E_m is the martensite Young's Modulus , ε_{my} is the martensite maximum elastic deformation, σ_m is the maximum stress in the martensite. The martensite mechanical behavior is illustrated in the fig. below:

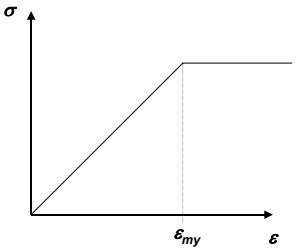

Figure 6: Martensite mechanical behaviour.

Considering then the case with 0<ξ< 1, the stress-strain relation is given by:

$$\sigma = \xi.\sigma_M + (1-\xi).\sigma_A \Rightarrow \begin{cases} \varepsilon = \dfrac{\sigma}{\xi.E_M + (1-\xi).E_A} & \text{for} \quad |\varepsilon| \le |\varepsilon_{my}| \\ \varepsilon = \dfrac{\sigma - \xi.Em.\varepsilon_{my}}{(1-\xi).E_A} & \text{for} \quad |\varepsilon| > |\varepsilon_{my}| \end{cases} \quad (5)$$

The dynamics of the actuator is now considered. A simplified diagram of the actuator and the main forces are shown in the Figure 7, where the coordinate *x* represents the position of the load.

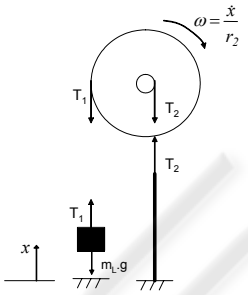

Figure 7: Diagram of the actuator and main forces.

The traction T_1 holds the load, T_2 is the traction acting on the SMA wire and ω is the angular velocity of the pulley. So, being *J* the moment of inertia of the pulley and m_L the mass of the load, using the basic laws of Mechanics one obtains:

$$-T_1.r_2 + T_2 r_1 = J.\frac{\ddot{x}}{r_2} \quad ; \quad -m_L g + T_1 = m_L.\ddot{x} \quad (6)$$

Traction T_2 may be estimated using a linear spring analogy. Figure 8 shows the wire in three possible states. In the austenite phase, the "spring" presents its initial length l_0. In the martensite phase, the wire reaches its maximum length l_{wire}, that correspond to the situation in which the load position is x=0. The difference between l_0 and l_{wire} is approximately 4% of the l_{wire}. In an intermediate phase, the "spring" elongation Δl is given by $4\%.l_{fio} - x/n$.

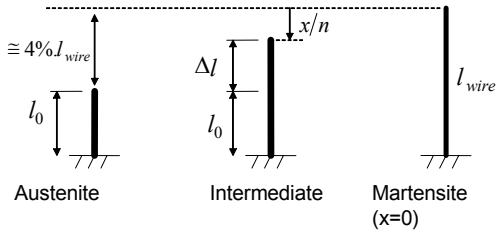

Figure 8: Spring analogy.

So, the traction is given by $T_2 = K.\Delta l = K.(0{,}04.l_{wire} - x/n)$, where K is the equivalent stiffness coefficient of the wire. Including a damping term, the equation of motion of the actuator becomes:

$$\left(J/r_2^{\,2} + m_L\right).\ddot{x} + c.\dot{x} + K/n^2.x = -m_L g + (0.04 l_{wire} K)/n \quad (7)$$

The stiffness coefficient K may be evaluated using (5). Assuming elastic behavior, being A_{wire} the sectional area of the wire, one obtains:

$$\sigma = \left[\xi.E_M + (1-\xi).E_A\right]\varepsilon \quad \text{or}$$

$$\frac{T_2}{A_{wire}} = \left[\xi.E_M + (1-\xi).E_A\right]\frac{\Delta l}{l_0} \quad (8)$$

Finally, considering that martensite stress will be higher than its elastic limit, it may be assumed that it will present a full plastic behavior, with a very small stiffness. So, E_M may be excluded from (8), resulting the approximation:

$$K = \left[(1-\xi).E_A\right]\frac{A_{wire}}{l_0} \quad (9)$$

4 PARAMETER IDENTIFICATION

Thermal parameters *C* and *h*, as well as the transformation temperatures (*Ms*, *Mf*, *As* and *Af*) must be accurately evaluated using a proper experimental procedure. A ramp excitation was induced in the wire, inducing a displacement of the load, as shown in Figure 9.

Using an optimization algorithm based on Quadratic Sequential Programming (SQP), the model parameters were adjusted in order to make the model to recover the measured position accurately. The following parameters were obtained,: *C*=0.255 W/ºC/m, *h*=7 W/m²ºC/m, Ms = 66ºC , Mf = 34ºC As = 53ºC, Af = 93ºC. The comparison between the measured position ant that obtained by the model simulation is given in Figure 10. A good accuracy of the model is verified.

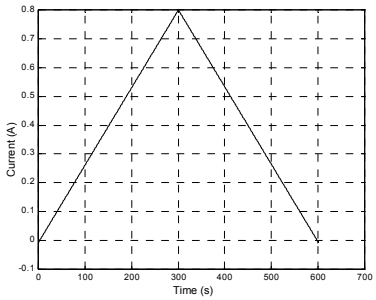

(a)

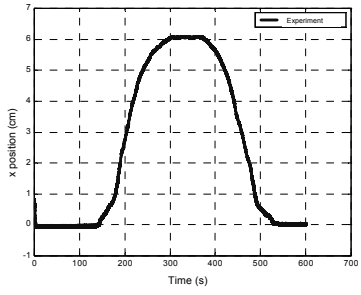

(b)

Figure 9: (a) Current ramp excitation; (b) Position of the load.

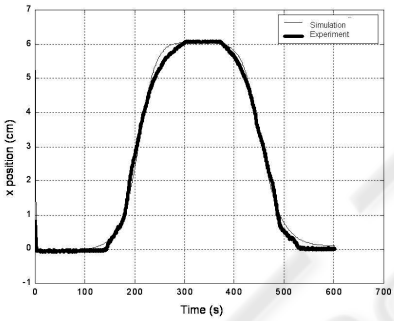

Figure 10 Comparison between simulation and experimental results

5 CONTROL SYSTEM DESIGN

In order to apply the sliding mode control to the SMA actuator, the model previously developed must be adapted, following the formulation exposed in Slotine and Li (1991). After some algebraic manipulation using (1) and (2), the dynamics of phase transformation can be written as:

$$\dot{\xi} = f(\xi) + b(\xi).u \tag{10}$$

with:

$$f(\xi) = \frac{-a}{\xi_0 mc_P}\left(\xi_0(\xi-k)-(\xi-k)^2\right)\left(hAT_{amb}+cT_P-(hA+c)\left(\frac{1}{a}\ln\left(\frac{\xi_0}{\xi-k}-1\right)+b\right)\right)$$

$$b(\xi) = \frac{-a}{\xi_0 mc_P}\left(\xi_0(\xi-k)-(\xi-k)^2\right)R \;;\; u = I^2$$

and

$$\begin{cases} a = \dfrac{6.2}{A_f - A_s}; b = \dfrac{A_s + A_f}{2}; \xi_0 = \xi_M; k = 0 \text{ if } \dot{T} > 0 \\ a = \dfrac{6.2}{M_s - M_f}; b = \dfrac{M_s + M_f}{2}; \xi_0 = 1 - \xi_A; k = \xi_A \text{ if } \dot{T} < 0 \end{cases}$$

Using (1) and (9), the dynamics of the motion can also be written as:

$$I\ddot{x} + c\dot{x} + \frac{K_0(1-\xi)}{n^2}x = -m_L g + \frac{K_0(1-\xi)}{n}\Delta \tag{11}$$

With $I = \left(J/r_2^{\,2} + m_L\right)$; $K_0 = E_A\, A_{wire}/l_0$ and $\Delta = 0.04 l_{wire}$. In equations (10) and (11), the variable x is measured, but the variable ξ must be estimated. This may be done considering a quasi-static approximation to (11), making $\dot{x} = \ddot{x} = 0$, that results:

$$\hat{\xi} = 1 - \frac{m_L g}{K_0\left(\dfrac{\Delta}{n} - \dfrac{x}{n^2}\right)} \tag{12}$$

Differentiating (11), and using (10), one obtains the SMA model adequate to apply sliding mode control, as proposed by Slotine and Li (1991):

$$\dddot{x} = f(\mathbf{x}) + b(\mathbf{x}).u \tag{13}$$

with $\mathbf{x} = \left(\xi \quad x \quad \dot{x} \quad \ddot{x}\right)^T$,

$$f(\mathbf{x}) = \frac{-c}{I}\ddot{x} - \frac{K_0(1-\xi)}{In^2}\dot{x} + \left(\frac{K_0 x}{In^2} - \frac{K_0\Delta}{In}\right)f(\xi)$$

and $b(\mathbf{x}) = \left(\dfrac{K_0 x}{In^2} - \dfrac{K_0\Delta}{In}\right)b(\xi)$.

So, the control action $u = i^2$ is given by:

$$u = \frac{1}{\hat{b}(\mathbf{x})}\left(-\hat{f}(\mathbf{x}) + \dddot{x}_d - 2\lambda\ddot{\tilde{x}} - \lambda^2\dot{\tilde{x}}\right) - K_{SM}\,sat(s/\phi) \tag{14}$$

with $s = \ddot{\tilde{x}} + 2\lambda\dot{\tilde{x}} + \lambda^2\tilde{x}$. $\hat{f}(\mathbf{x})$ and $\hat{b}(\mathbf{x})$ are the best estimates of the functions in model (13), considering the approximate values for the parameters and the estimate of the variable ξ given in (12). x_d is the desired position of the actuator load (set-point), λ is a positive constant related to the cut-off frequency of the closed-loop system, ϕ is the boundary layer thickness to avoid control chattering and K_{SM} is a control gain related to the modeling and parameter estimation errors. A detailed description of the control design may be found in Slotine and Li (1991).

6 EXPERIMENTAL RESULTS

The control logic previously developed was applied to the experimental prototype, and the performance

of the closed loop system could be evaluated. Figure 11 shows a reference step of 2.5cm applied at t=10s. Control parameters are λ=40; ϕ=1,6 and K_{SM}=64. The 5% settling time obtained is 0,23s, and the maximum overshoot is 0,6%.

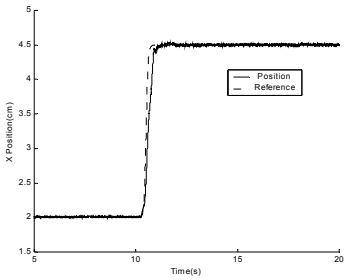

Figure 11: Step response of the SMA actuator.

A harmonic set-point was applied to the actuator, with amplitude of 1cm and periods of 20s and 5s (Figure 12. It can be seen that, despite a small oscillation around the set-point, the system follows the reference with good accuracy. Tests with decreasing periods indicated a 0.69Hz cut-off frequency, despite of a 0.37Hz obtained with a conventional PID controller. Finally, a cooling disturbance was applied, created by a computer cooler fan directed toward the SMA wire (Figure 13). The robustness of the controller can be verified, by comparing the response with the open-loop response.

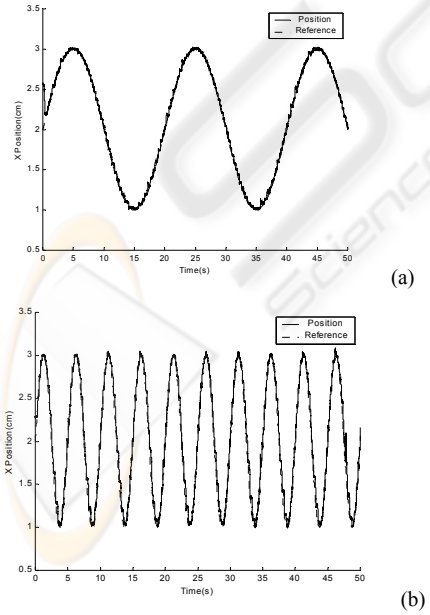

Figure 12: Harmonic set-point response of the SMA actuator (cm amplitude). (a) 20s; (b) 5s period

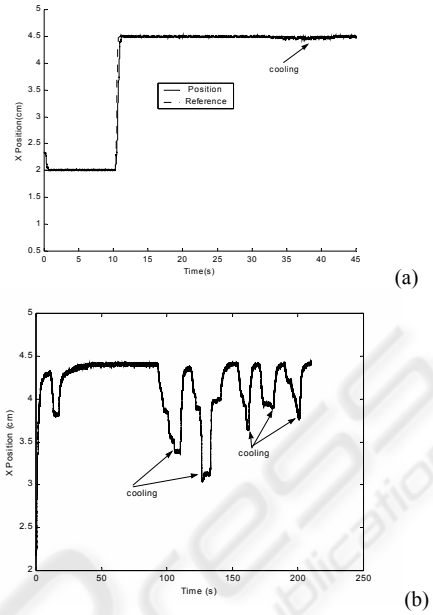

Figure 13: Cooling disturbance response of the SMA actuator (a) closed-loop; (b) opened-loop

7 CONCLUSIONS

A novel SMA actuator was proposed, using the thermoelectric effect for cooling the SMA wire. An experimental prototype was built, and a mathematical model was developed. The model parameters were adjusted by means of an experimental identification procedure. The validated model was then used to design a sliding mode controller. Such controller is able to deal with model and parameter uncertainties, and also with non-linear effects. Closed-loop preliminary results obtained in the experimental set-up showed that the proposed actuator presents a good dynamic response and low sensibility to disturbs of load and ambient cooling. So it is recommended in application with SMA devices.

ACKNOWLEDGEMENTS

The authors would like to express their gratitude for the IPT (Institute for Technological Research - São Paulo, Brazil) for supporting this research and for CNPq (National Council for Scientific and Technological Development), Research Process Number 484232/2006-1.

REFERENCES

Asada, H.H. and Mascaro S., 2002, “Wet Shape Memory Alloy Actuators”, MIT Home Automation and Healthcare Consortium, Phase 3 Final Report, Boston, USA.

Ashrafiuon, H. and Elahinia H.M., 2002, “Nonlinear Control of a Shape Memory Alloy Actuated Manipulator”, ASME Journal of Vibration and Acoustics, Vol. 124, pp.566-575.

Dutta, S.M. and Ghorbel, F.H., 2005, "Differential Hysteresis Modeling of a Shape Memory Alloy Wire Actuator," IEEE/ASME Transactions on Mechatronics, Vol. 10, Issue 2, April , pp. 189-197.

Dynalloy, Inc., 2005, “Flexinol – Wire specifications”. Available at: http:// www.dynalloy.com. Acess: 20 Dec. 2005.

Furuya, Y. and Shimada H., 1990, “Shape Memory Actuator for Robotic Applications, Engineering Aspect of Shape Memory Alloys”, Butterworth-Heinemann, London, pp 338-355.

Gorbet, B.R. and Russel A.R., 1995, “Improve the Response of SMA Actuators”, IEEE International Conference on Robotic and Automation, Vol. 3, May, pp. 2299-2303.

Grant, D., Hayward V. and Lu A., 1997, “Design and Comparison of High Strain Shape Memory Alloy Actuators”, International Conference on Robotic and Automation, Albuquerque, New Mexico, 260-265.

Hoder K., Vasina, M. and Solc F., 2003, “Shape Memory Alloy- Unconventional Actuators”, International Conference on Industrial Technology ICIT, Maribor, Slovenia, pp. 190-193.

Ikuta K., Tsukamoto M. And Hirose, S., 1991, “Mathematical Model and Experimental Verification of Shape Memory Alloy for Designing Micro Actuator”, Proc. of the IEEE on Micro Electromechanical Systems, an Investigation of Microstructures, Sensors, Actuators, Machines, and Robots, pp.103-108.

Incropera, P.F. and Witt, D.P.D., 1998, “Fundamentos de transferência de calor e de massa”, 4 ed., Rio de Janeiro, LTC (In Portuguese).

Slotine, J.J.E. and Li, W., 1991, “Applied nonlinear control”, Englewood Cliffs: Prentice –Hall, USA.

Tanaka,Y. and Yamada Y., 1991, “A Rotary Actuator Using Shape Memory Alloy for a Robot, and Analysis of the Response with Load”, IEEE/RSJ International Workshop on Intelligent Robots and Systems IROS ’91, Osaka, Japan, pp1163-1168.